RESEARCH LETTER

Comparison of the effects of silver phosphate and selenium nanoparticles on *Staphylococcus aureus* growth reveals potential for selenium particles to prevent infection

Dagmar Chudobova[1], Kristyna Cihalova[1], Simona Dostalova[1], Branislav Ruttkay-Nedecky[1,2], Miguel Angel Merlos Rodrigo[1,2], Katerina Tmejova[1,2], Pavel Kopel[1,2], Lukas Nejdl[1], Jiri Kudr[1], Jaromir Gumulec[1,3], Sona Krizkova[1,2], Jindrich Kynicky[1,2], Rene Kizek[1,2] & Vojtech Adam[1,2]

[1]Central European Institute of Technology, Brno University of Technology, Brno, Czech Republic; [2]Department of Chemistry and Biochemistry, Faculty of Agronomy, Mendel University in Brno, Brno, Czech Republic; and [3]Department of Pathological Physiology, Faculty of Medicine, Masaryk University, Brno, Czech Republic

Correspondence: Vojtech Adam, Department of Chemistry and Biochemistry, Mendel University in Brno, Zemedelska 1, CZ-613 00 Brno, Czech Republic.
Tel.: +420 545 133 350;
fax: +420 545 212 044;
e-mail: vojtech.adam@mendelu.cz

Received 30 October 2013; revised 25 November 2013; accepted 3 December 2013. Final version published online 30 December 2013.

DOI: 10.1111/1574-6968.12353

Editor: Jeff Cole

Keywords
antimicrobial effect; growth; inhibition; nanotechnology.

Abstract

Interactions of silver phosphate nanoparticles (SPNPs) and selenium nanoparticles (SeNPs) with *Staphylococcus aureus* cultures have been studied at the cellular, molecular and protein level. Significant antibacterial effects of both SPNPs and SeNPs on *S. aureus* were observed. At a concentration of 300 μM, SPNPs caused 37.5% inhibition of bacterial growth and SeNPs totally inhibited bacterial growth. As these effects might have been performed due to the interactions of nanoparticles with DNA and proteins, the interaction of SPNPs or SeNPs with the amplified *zntR* gene was studied. The presence of nanoparticles decreased the melting temperatures of the nanoparticle complexes with the *zntR* gene by 23% for SeNPs and by 12% for SPNPs in comparison with the control value. The concentration of bacterial metallothionein was 87% lower in bacteria after application of SPNPs (6.3 μg mg^{-1} protein) but was increased by 29% after addition of SeNPs (63 μg mg^{-1} protein) compared with the *S. aureus* control (49 μg mg^{-1} protein). Significant antimicrobial effects of the nanoparticles on bacterial growth and DNA integrity provide a promising approach to reducing the risk of bacterial infections that cannot be controlled by the usual antibiotic treatments.

Introduction

Staphylococcus aureus is often a cause of infection in vascular grafts. Such infection may treated with appropriate antibiotics, but most *S. aureus* strains have developed resistance to available antibiotics, and resistance even to new antibiotics is steadily growing (van Hal & Fowler, 2013). The use of metal-based drugs and nanoparticles is one of the highly promising means to suppress infections caused by antibiotic-resistant bacteria (Rai *et al.*, 2009). Synthesized silver and selenium nanoparticles (SeNPs) have been found to be bactericidal and have been proved to be good alternatives for the development of antimicrobial agents (Tran & Webster, 2011; Wang & Webster, 2013). Metallic nanoparticles interacting with cellular components (DNA, RNA and ribosomes) deactivate and effectively alter cellular processes (Grigor'eva *et al.*, 2013). It is assumed that silver nanoparticles can penetrate the cell membrane to reach the cytosol due to their ability to dissolve slowly while releasing Ag^+ ions, but the exact mechanism of the silver nanoparticles antimicrobial action remains unclear.

Selenium has been studied for various medical applications and as a potential material for orthopaedic implants (Wang & Webster, 2012). There also are studies indicating an ability of selenium compounds to inhibit the growth of bacteria and the formation of bacterial biofilms (Wang & Webster, 2012). Among numerous selenium compounds, 2,4,6-tri-para-methoxyphenylselenopyrylium chloride, 9-para-chlorophenyloctahydroselenoxanthene, and perhydroselenoxanthene have been demonstrated to have antibacterial activity *in vitro*, especially against *S. aureus*.

FEMS MICROBIOLOGY LETTERS

However, the precise effect of elemental SeNPs remains largely unknown (Tran & Webster, 2011; Ramos *et al.*, 2012).

In the past decade, study of the toxicological properties of nanomaterials and/or nanoparticles has opened up a new research field known as nanotoxicology (Yan *et al.*, 2013). Research on nanotoxicity is of extremely high scientific, social and economic value (Pumera, 2011). Nanomaterial-induced reactive oxygen species play a key role in cellular and tissue toxicity (Yan *et al.*, 2013). The toxicity of silver nanoparticles is enhanced in the presence of H_2O_2, highlighting the biological relevance of investigating the oxidative dissolution of these nanoparticles (Ho *et al.*, 2010). In addition, it has been shown that SeNPs can inhibit proliferation and induce apoptosis in promastigote forms of the protozoa *Leishmania major* (Beheshti *et al.*, 2013).

The aims of this study were to investigate the effects of SeNPs and silver phosphate nanoparticles (SPNPs) on inhibiting growth in *S. aureus*, morphologically altering the bacteria cell structure and changing its biochemical parameters, and thereby to identify a suitable substance with antibacterial properties to reduce the risk of bacterial (staphylococcal) infections. Another focus was to observe effects of both SeNPs and SPNPs on bacterial metallothionein concentration and to study the interactions of these nanoparticles with the amplified *zntR* gene.

Materials and methods

Cultivating *S. aureus*

Staphylococcus aureus (NCTC 8511) was obtained from the Czech Collection of Microorganisms, Masaryk University, CZ. *Staphylococcus aureus* was inoculated into lysogeny broth medium for 24 h on a shaker at 40 ***g*** and 37 °C. The bacterial culture was diluted to $OD_{600\ nm} = 0.1$ for all experiments. Petri dishes were each covered with 3 mL of the *S. aureus* culture in lysogeny broth that had been grown for 24 h. Discs 1 cm in diameter applied to Petri dishes with bacteria were cut out from vascular grafts produced by the VUP Medical (Czech Republic) and were mixed with SPNPs or SeNPs in various concentrations. Dishes were incubated in a growth chamber at 37 °C for 24 h. Growth was measured by absorbance using a Multiskan EX apparatus (Thermo Fisher Scientific, Germany). For measurement purposes, *S. aureus* culture was mixed in the microplate with various concentrations of SPNPs and SeNPs. As a control, the culture was also grown without nanoparticles. The concentrations of SPNPs or SeNPs were 0, 10, 25, 50, 75, 150, 225 and 300 μM. Total volume in the microplate wells was always 300 μL (Chudobova *et al.*, 2013a, b).

Analysing biochemical parameters of *S. aureus*

The effect of nanoparticles on *S. aureus* was tested using STAPHYtest 24 biochemical detection tests (Erba Lachema, Czech Republic) for the following substances: urease, arginine, ornithine, β-galactosidase, β-glucuronidase, β-glucosidase, phosphatase, esculin, *N*-acetyl-β-D-glucosamine, sucrose, mannitol, xylose, galactose, trehalose, maltose, mannose, lactose, sorbitol, ribose, fructose, cellobiose, arabinose, xylitol and raffinose. Substances were mixed with *S. aureus* bacterial culture with or without added nanoparticles (300 μM). Complexes were measured for 24 h using the Multiskan EX apparatus via ASCENT Software for Multiskan.

Preparing and characterizing SPNPs and SeNPs

SPNPs were prepared by dissolving (di)sodium hydrogen phosphate heptahydrate in water purified to the American Chemical Society (ACS) standard and then adding a solution of SPNPs nitrate in ACS-standard water according to Khan *et al.* (2012). The reaction proceeded immediately with the formation of yellow colloidal nanoparticles (200–300 nm in diameter; Chudobova *et al.*, 2013a, b). To the prepared SeNPs, sodium selenite pentahydrate $Na_2SeO_3{\cdot}5H_2O$ (26.3 mg) was dissolved in 50 mL ACS-standard water, and 3-mercaptopropionic acid (40 μL) was then slowly added to the solution under stirring. Afterwards, pH was adjusted to eight using 1 M NaOH. The reaction mixture was stirred for 2 h. SeNPs were stored in darkness at 4 °C. One millilitre of the solution contains 158 μg of Se nanoparticles (50–100 nm in diameter). Chemicals used in this study were purchased from Sigma-Aldrich in ACS purity unless noted otherwise.

SPNPs and SeNPs were measured on a Spectro Xepos spectrometer (Spectro Analytical Instruments, Germany). The samples were measured on a powder diffraction anode X-ray tube at 47.63 kV and 0.5 mA current and were detected with a Barkla scatter aluminium oxide. The sample was measured through the polyethylene bottle side wall 20 mm above the bottom. The SPECTRO XEPOS software and TurboQuant method were applied for data analysis.

Cell microscopy

An Olympus IX 71 inverted system microscope (Japan) was used for imaging of the cells. Total magnification was 1600×. The parameters included an exposure time of 32 ms and ISO was set to 200. Structures were also characterized using an FEG-SEM MIRA XMU electron microscope (Tescan, Czech Republic). Samples were coated with 10 nm of carbon using a K950X carbon coater (Quorum Technologies, UK). For automated acquisition

of selected areas, the TESCAN IMAGE SNAPPER proprietary software tool was used.

Determining total proteins

Pyrogallol red protein assay (Skalab, Czech Republic) is based upon the formation of a blue protein-dye complex in the presence of molybdate under acidic conditions (pH 2.5). 150 μL of the reagent mixture (50 mM succinic acid, 3.47 mM sodium benzoate, 0.06 mM sodium molybdate, 1.05 mM sodium oxalate, and 0.07 mM pyrogallol red) was pipetted into a plastic cuvette. Then, 8 μL of sample was added. Absorbance was measured at $\lambda = 605$ nm using a BS-400 chemistry analyser (Mindray, China) after 6 min of incubation. The resulting value was calculated from the absorbance values of the pure reagent mixture and that of the sample after 6 min of incubation.

Differential pulse voltammetric determination of metallothionein

Electrochemical measurements were performed on a 747 VA Stand instrument connected to a 746 VA Trace Analyzer and 695 Autosampler (Switzerland), using a standard cell with three electrodes and cooled sample holder (4 °C). As a supporting electrolyte, Brdicka solution containing 1 mM $Co(NH_3)_6Cl_3$ and 1 M ammonium buffer [$NH_3(aq)$ and NH_4Cl, pH 9.6] was used (Adam *et al.*, 2008).

Interaction of *zntR* gene from DNA with SPNPs and SeNPs

The *zntR* gene was amplified from *S. aureus* according to Singh *et al.* (1999). Spectra were recorded at 200–400 nm after 120 min of interaction using 1-cm quartz cuvettes (Hellma, UK) on a SPECORD 210 spectrophotometer (Analytik Jena, Germany) at 25 °C. Denaturation of a complex of amplified *zntR* gene with SPNPs and SeNPs in eight concentrations (0, 10, 25, 50, 75, 150, 225 and 300 μM) was monitored spectrophotometrically using a SPECORD S600 spectrophotometer with a diode detector (Analytik Jena). The sample was incubated for 3 min at increasing temperatures at 25–99 °C and the absorbance was measured at 200–800 nm.

Determining protein mass spectra by matrix-assisted laser desorption/ionization time of flight (MALDI-TOF)

After cultivation overnight, 500 μL culture ($0.1 = OD_{600\ nm}$) was centrifuged at 14 000 ***g*** for 2 min. Supernatant was discarded and the pellet was suspended in 300 μL of deionized water. Then, 900 μL of ethanol was added. After centrifugation at 14 000 ***g*** for 2 min, the supernatant was discarded and the obtained pellet was air-dried. The pellet was then dissolved in 25 μL of 70% formic acid (v/v) and 25 μL of acetonitrile and mixed. The samples were centrifuged at 14 000 ***g*** for 2 min and 1 μL of the clear supernatant was spotted in duplicate onto an MTP 384 target (Bruker Daltonics) and air-dried at room temperature. Each spot was overlaid with 1 μL of α-cyano-4-hydroxycinnamic acid matrix solution. Spectra were measured on a Bruker MALDI-TOF/TOF apparatus in the *m*/*z* range of 2–20 kDa.

Results

Metal nanoparticles caused significant growth inhibition of *S. aureus*, with application of SeNPs inducing twice as much growth inhibition as SPNPs (7.0 ± 0.5 and 3.0 ± 0.5 mm, respectively). There were also significant morphological changes in the cell structure, these being most evident in the nucleoid (Fig. 1A).

In addition, our synthesized nanoparticles (SPNPs or SeNPs) were characterized with a scanning electron microscope (Fig. 1B). Figure 1(B-d) shows the structure of *S. aureus* culture without the addition of nanoparticles. In the case of SPNPs, the formations were square or spherical in character (Fig. 1B-e) and in the case of SeNPs only small spherical particles (Fig. 1B-f) were observed, which confirmed our previous hypothesis.

After *S. aureus* had been exposed for 18 h to SPNPs, inhibition of bacterial growth was observed and absorbance values at 600 nm had decreased from 0.4 to 0.25 a.u. (Fig. 2A-a). In applying the SPNP concentration with the weakest antibacterial activity (10 μM) to the bacterial culture, absorbance values comparable to those of the control group (0.4) were obtained. The greatest decrease in absorbance values (by 38%) in comparison with the control was achieved by applying 300 μM SPNPs (Fig. 2A-a). By contrast, in the case of SeNPs, the minimum inhibitory concentration was achieved when 10 μM SeNPs was applied and the total inhibitory concentration occurred when 300 μM SeNPs was applied (Fig. 2A-b). Half maximal inhibitory concentration values confirmed the obtained results, as IC_{50} was 268.2 for SPNPs and 4.4 μM for SeNPs.

We also investigated changes in the biochemical parameters of *S. aureus* after the addition of nanoparticles. Twenty-four hours after application of SPNPs (300 μM), changes in 11 biochemical tests (of 24 tests in total) were observed (Fig. 2B-b). After application of SeNPs, the results of only seven tests were different from those of the control group (Fig. 2B-c).

Because we observed changes in the morphology of the bacterial cell nucleoid after exposure of *S. aureus* to

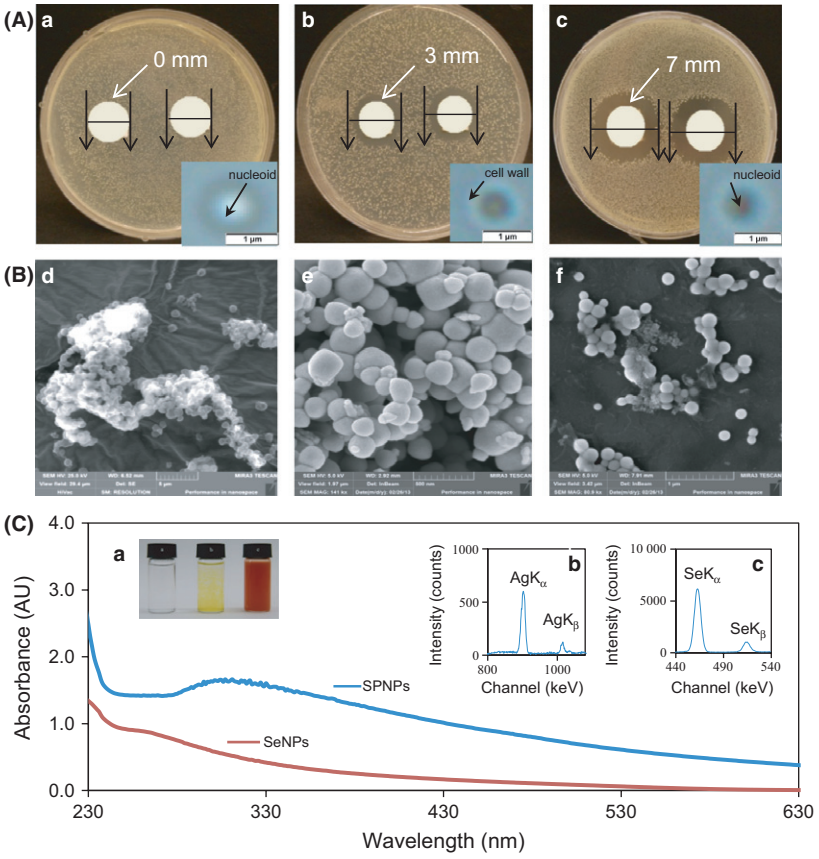

Fig. 1. (A) Growth inhibition zones in bacterial culture after application of 300 μM of nanoparticles and a microscopic view of cells: (a) *Staphylococcus aureus*, (b) after application of SPNPs, (c) after application of SeNPs. (B) Bacterial culture and nanoparticles under electron microscopy: (d) *S. aureus*, (e) SPNPs, (f) SeNPs. Images are in different scales, with 1 unit of the scale corresponding to 5 μm in B-d, 500 nm in B-e, and 1 μm in B-f. (C) Absorption spectra of 300 μM of SPNPs and SeNPs: (a) visualization in ambient light: MilliQ water, SPNPs, SeNPs; X-ray view of content elements: (b) SPNPs; (c) SeNPs.

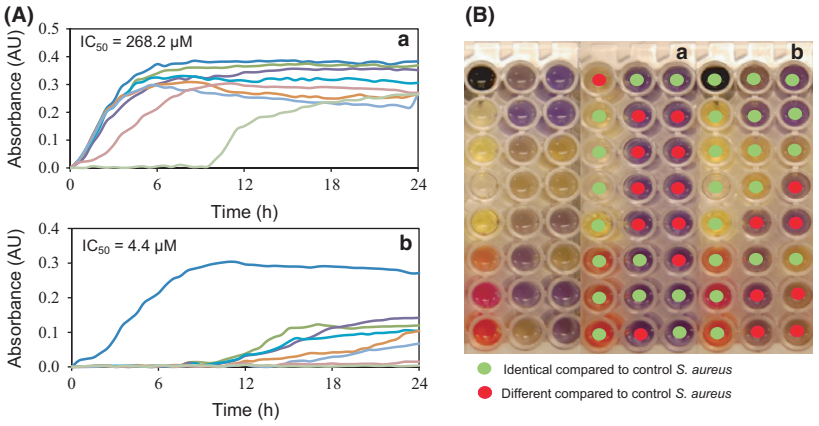

Fig. 2. (A) Spectrophotometric analysis of the growth of *S. aureus* bacterial culture with (a) SPNPs and (b) SeNPs in concentrations 0, 10, 25, 50, 75, 150, 225 and 300 μM. (B) Biochemical parameters of (a) *S. aureus*, (b) *S. aureus* with 300 μM SPNPs, and (c) *S. aureus* with 300 μM SeNPs.

SPNPs or SeNPs, we investigated the interaction of both nanoparticle types with DNA using amplified *zntR* gene. After application of the various concentrations of SeNPs (0, 10, 25, 50, 75, 150, 225 and 300 μM) there was a marked increase in absorbance signal at 260 nm with increasing concentrations of SeNPs (Fig. 3A-b) and composition of nanoparticles, but this shift was not observed when SPNPs were applied (Fig. 3A-a). Statistically significant changes were observed in the melting temperatures of the amplified *zntR* gene in complexes with SPNPs or SeNPs at the highest concentration of 300 μM (Fig. 3B). Differential changes in the melting temperature of amplified *zntR* gene probably can be caused by different affinity of nanoparticles to the bacterial DNA. A greater decrease in melting temperature in comparison with the control was observed in the interaction of SPNPs and amplified *zntR* gene, than in the interaction of SeNPs with amplified *zntR* gene (23% vs. 12%, respectively). SPNPs may

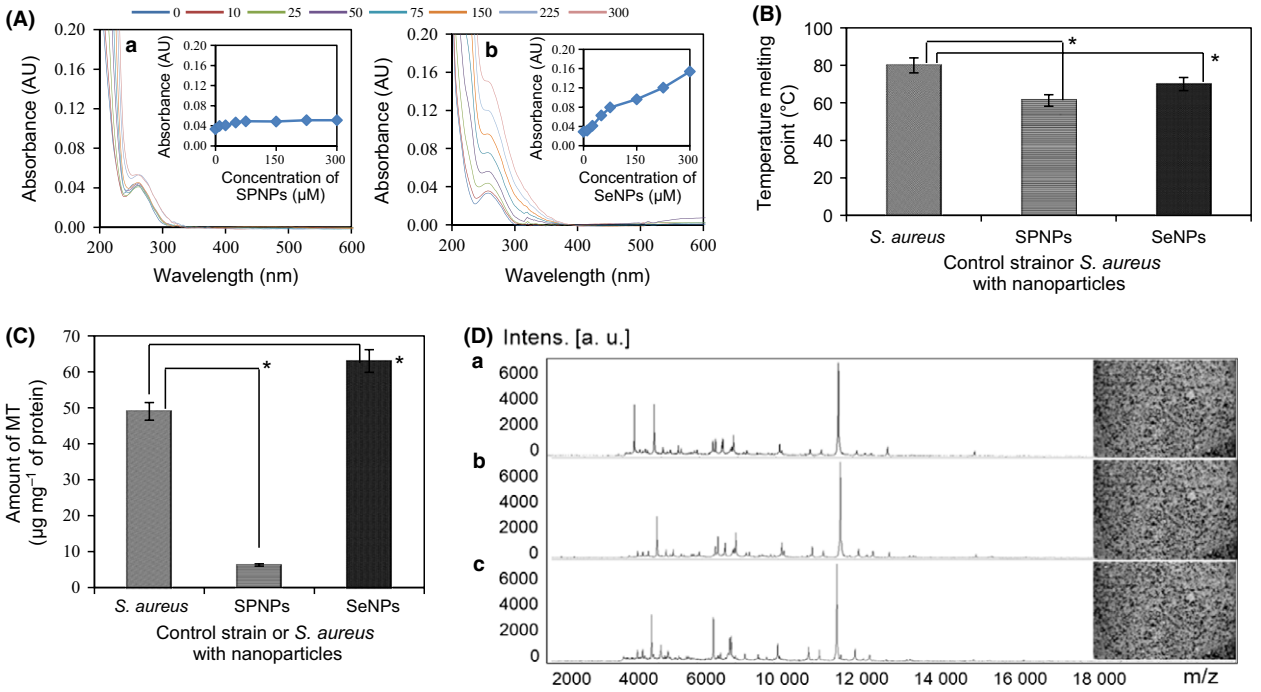

Fig. 3. (A) Spectrophotometric determination of amplified *zntR* gene after application of different concentrations (0, 10, 25, 50, 75, 150, 225 and 300 μM) of nanoparticles: (a) SPNPs, (b) SeNPs. (B) Changes of bacterial DNA melting temperature after application of SPNPs and SeNPs. (C) Determination of metallothionein in control strain and after application of silver and SeNPs. (B and C) Data represent the mean ± SD from three measurements, $*P < 0.05$. (D) MALDI-TOF mass spectra protein fingerprints for the identification of (a) *Staphylococcus aureus* and *S. aureus* after application of (b) SPNPs or (c) SeNPs.

have a greater affinity for the amplified *zntR* gene than SeNPs.

The concentration of bacterial metallothionein was significantly lower (by about 87%) in bacterial cells after application of SPNPs (6.3 μg mg^{-1} protein) and a higher (about 29%) concentration of metallothionein occurred in bacterial cells after addition of SeNPs (63 μg mg^{-1} protein) as compared with the *S. aureus* control (49 μg mg^{-1} protein; Fig. 3C). The presence of the *zntR* gene, which encodes metallothionein formation, was confirmed by polymerase chain reaction (results not shown). The effect of nanoparticles probably caused a change in the protein composition of the *S. aureus* culture, as was demonstrated by MALDI-TOF mass spectrometry, although the change was not statistically significant (Fig. 3D).

Discussion

Advances in nanotechnology, and particularly in the preparation of metal nanoparticles, can be considered to constitute one of the keys to developing new vascular grafts, because silver ions can lead to the prevention of bacterial infection (Ho *et al.*, 2013). In addition, SeNPs have been found to have high antibacterial activity and they can be easily prepared (Ramos *et al.*, 2012). The antibacterial activity of SeNPs was greater than that of the SPNPs used in this study, and it was comparable to that of the smaller SPNPs (18–21 nm) used by Prabakar *et al.* (2013). This probably was because we prepared SeNPs that were smaller in size (50–100 nm) than the SPNPs (200–300 nm). The present study showed that the silver nanoparticles exhibited antibacterial activity even at nanoparticle sizes equal to hundreds of nm. When comparing our findings on inhibition of *S. aureus* growth in the presence of selenium to those from other scientists, we found that our results were similar to those of Naik *et al.* (2009). However, our colonies were smaller than those of Naik *et al.*, probably because they had used selenium in a complex with 2-selenobenzo[*h*]quinoline-3-carbaldehyde.

The effect of 40–60 nm SeNPs on *S. aureus* was studied by Tran & Webster (2011). In that work, bacterial growth was inhibited by SeNPs in the concentration range 7.8–31 μg mL^{-1} to approximately 1.7% of that seen in the controls and the SeNPs killed approximately 40% of *S. aureus* cells. Antimicrobial activity of SeNPs was also confirmed in the work of Hariharan *et al.* (2012).

In our study the highest used concentration of SeNPs (300 μM, 23.7 μg mL^{-1}) caused total growth inhibition

within 24 h. Similar results for a 24-h inhibition period in relation to *S. aureus* growth on selenium nanoparticle-coated polyvinyl chloride are presented in the work of Ramos *et al.* (2012). The most interesting finding of our study is that the total inhibition concentration of SeNPs should be at least 5 μg mL^{-1}, which corresponds with results published by Tran & Webster (2011). Biochemical parameters showed greater similarity between *S. aureus* with the addition of SeNPs and the control, but greater differences with the addition of SPNPs.

Our study also demonstrated the interaction of DNA with SeNPs, whereby these particles probably impair the DNA structure of the *zntR* gene amplified *in vitro*. This statement is supported by the study of Beheshti *et al.* (2013), which reported increasing concentrations of SeNPs biosynthesized by *Bacillus* sp. MSH-1-induced cytotoxic effects and apoptosis in promastigote forms of the protozoa *L. major*. Apoptosis was demonstrated by DNA fragmentation in the concentration range 1–150 μg mL^{-1} of SeNPs. A similar toxicity effect of SeNPs on genomic DNA had been reported by Chen *et al.* (2008) for human melanoma cells treated with chemically synthesized SeNPs. Treatment of A375 human melanoma cells with SeNPs resulted in dose-dependent cell apoptosis, as indicated by DNA fragmentation and phosphatidylserine translocation (Chen *et al.*, 2008).

In our study, the results regarding concentration of metallothionein were comparable to those of Dar *et al.* (2013). Their group was interested in the production of metallothionein in various microorganisms in response to cadmium and they showed an increased accumulation of cadmium in cells expressing the protein metallothionein in comparison with control cells. Our results show a distinct decrease in metallothionein synthesis after addition of SPNPs to *S. aureus*. In contrast, only a slight increase was observed after the addition of SeNPs. This may be associated with a similarity in the biochemical parameters of *S. aureus* with and without the addition of SeNPs. After the addition of SPNPs, *S. aureus* showed more differences in biochemical parameters. After application of both SPNPs and SeNPs, on the other hand, *S. aureus* bacterial culture showed only minor differences in MALDI-TOF mass spectra protein fingerprints in comparison with the control. This leads to the conclusion that smaller nanoparticles (SeNPs) have a greater inhibitory effect compared with larger nanoparticles (SPNPs). Our results suggest an effective way to prevent *S. aureus* infections using nanostructured selenium.

Acknowledgements

Financial support from Sensor, Information and Communication Systems CZ.1.05/2.1.00/03.0072 is gratefully acknowledged. The authors declare no conflict of interest.

References

Adam V, Baloun J, Fabrik I, Trnkova L & Kizek R (2008) An electrochemical detection of metallothioneins at the zeptomole level in nanolitre volumes. *Sensors* **8**: 2293–2305.

Beheshti N, Soflaei S, Shakibaie M, Yazdi MH, Ghaffarifar F, Dalimi A & Shahverdi AR (2013) Efficacy of biogenic selenium nanoparticles against *Leishmania major*. *In vitro* and *in vivo* studies. *J Trace Elem Med Biol* **27**: 203–207.

Chen T, Wong YS, Zheng W, Bai Y & Huang L (2008) Selenium nanoparticles fabricated in *Undaria pinnatifida* polysaccharide solutions induce mitochondria-mediated apoptosis in A375 human melanoma cells. *Colloids Surf B Biointerfaces* **67**: 26–31.

Chudobova D, Dobes J, Nejdl L *et al.* (2013a) Oxidative stress in *Staphylococcus aureus* treated with silver(I) ions revealed by spectrometric and voltammetric assays. *Int J Electrochem Sci* **8**: 4422–4440.

Chudobova D, Nejdl L, Gumulec J *et al.* (2013b) Complexes of silver(I) ions and silver phosphate nanoparticles with hyaluronic acid and/or chitosan as promising antimicrobial agents for vascular grafts. *Int J Mol Sci* **14**: 13592–13614.

Dar S, Shuja RN & Shakoori AR (2013) A synthetic cadmium metallothionein gene (PMCd1syn) of *Paramecium* species: expression, purification and characteristics of metallothionein protein. *Mol Biol Rep* **40**: 983–997.

Grigor'eva A, Saranina I, Tikunova N, Safonov A, Timoshenko N, Rebrov A & Ryabchikova E (2013) Fine mechanisms of the interaction of silver nanoparticles with the cells of *Salmonella typhimurium* and *Staphylococcus aureus*. *Biometals* **26**: 479–488.

Hariharan H, Al-Dhabi NA, Karuppiah P & Rajaram SK (2012) Microbial synthesis of selinium nanocomposite using *Saccharomyces cerevisiae* and its antimicrobial activity against pathogens causing nosocomial infection. *Chalcogenide Lett.* **9**: 509–515.

Ho CM, Yau SKW, Lok CN, So MH & Che CM (2010) Oxidative dissolution of silver nanoparticles by biologically relevant oxidants: a kinetic and mechanistic study. *Chem Asian J* **5**: 285–293.

Ho CH, Odermatt EK, Berndt I & Tiller JC (2013) Long-term active antimicrobial coatings for surgical sutures based on silver nanoparticles and hyperbranched polylysine. *J Biomater Sci Polym Ed* **24**: 1589–1600.

Khan A, Qamar M & Muneer M (2012) Synthesis of highly active visible-light-driven colloidal silver orthophosphate. *Chem Phys Lett* **519–20**: 54–58.

Naik HRP, Naik HSB, Naik TRR, Naika HR, Gouthamchandra K, Mahmood R & Ahamed BMK (2009) Synthesis of novel benzo(*h*)quinolines: Wound healing, antibacterial, DNA binding and *in vitro* antioxidant activity. *Eur J Med Chem* **44**: 981–989.

Prabakar K, Sivalingam P, Rabeek SIM *et al.* (2013) Evaluation of antibacterial efficacy of phyto fabricated silver nanoparticles using *Mukia scabrella* (Musumusukkai) against

drug resistance nosocomial gram negative bacterial pathogens. *Colloid Surf B Biointerfaces* **104**: 282–288.

Pumera M (2011) Nanotoxicology: the molecular science point of view. *Chem Asian J* **6**: 340–348.

Rai M, Yadav A & Gade A (2009) Silver nanoparticles as a new generation of antimicrobials. *Biotechnol Adv* **27**: 76–83.

Ramos JF, Tran PA & Webster TJ (2012) *Selenium Nanoparticles for the Prevention of PVC-related Medical Infections*. Bioengineering Conference (NEBEC), 38th Annual Northeast March 2012.

Singh VK, Xiong AM, Usgaard TR, Chakrabarti S, Deora R, Misra TK & Jayaswal RK (1999) ZntR is an autoregulatory protein and negatively regulates the chromosomal zinc resistance operon znt of *Staphylococcus aureus*. *Mol Microbiol* **33**: 200–207.

Tran PA & Webster TJ (2011) Selenium nanoparticles inhibit *Staphylococcus aureus* growth. *Int J Nanomed* **6**: 1553–1558.

van Hal SJ & Fowler VG (2013) Is it time to replace vancomycin in the treatment of methicillin-resistant *Staphylococcus aureus* infections? *Clin Infect Dis* **56**: 1779–1788.

Wang Q & Webster TJ (2012) Nanostructured selenium for preventing biofilm formation on polycarbonate medical devices. *J. Biomed. Mater. Res. A* **100A**: 3205–3210.

Wang Q & Webster TJ (2013) Short communication: inhibiting biofilm formation on paper towels through the use of selenium nanoparticles coatings. *Int J Nanomed* **8**: 407–411.

Yan L, Gu ZJ & Zhao YL (2013) Chemical mechanisms of the toxicological properties of nanomaterials: generation of intracellular reactive oxygen species. *Chem Asian J* **8**: 2342–2353.